

The Variation in Flow Stress and Microstructure during Superplastic Deformation of the Al-Cu Eutectic

B. M. WATTS, M. J. STOWELL

Tube Investments Research Laboratories, Hinxton Hall, Saffron Walden, Essex, UK

with an Appendix by

D. M. COTTINGHAM* and B. M. WATTS

Stress-strain curves have been obtained for the superplastically deformed Al-Cu eutectic tested in tension under constant true strain-rate conditions. It is shown that constant flow stress conditions do not obtain and that, after an initial transient, the flow stress is linearly related to natural tensile strain. Optical metallography has been employed to follow the variation of both inter-phase particle separation and α -Al grain size with strain and it is concluded that the observed strain hardening is due mainly to grain coarsening.

1. Introduction

Superplastic deformation is obtained in certain alloy systems at temperatures above about half their melting point. It manifests itself as large, neck-free elongations which can be correlated with an unusually high value of the strain-rate-sensitivity, m [1] ($m = \partial \log \sigma / \partial \log \dot{\epsilon}$ where σ is the flow stress and $\dot{\epsilon}$ the true strain-rate). There is considerable information on the relationship between flow stress and strain-rate as a function of initial grain size [2-10]. Less common [7, 11], are quantitative studies of the microstructural changes occurring during deformation and their effect upon the flow stress, although some authors [12, 13] have noticed enhanced coarsening within the deformed regions.

The main object of the research described, which is a continuation of that reported earlier [14], was to investigate quantitatively the effect of strain and strain-rate upon the flow stress and microstructure of the Al-33 wt % Cu eutectic alloy during superplastic deformation. This alloy contains approximately equal volumes of the intermetallic phase CuAl_2 and the Al-rich (α) solid solution. The degenerate eutectic structure, if obtained on a sufficiently fine scale, is superplastic under specific testing conditions [14, 15].

2. Experimental Procedure

The alloy was prepared from super-pure

aluminium, supplied by British Aluminium Co Research Laboratories, and super-purity copper from Johnson Matthey & Co. Most of the experiments were performed on material which was vacuum-melted and chill-cast into a graphite mould of 67 mm diameter and 89 mm length. The as-cast billet was directionally re-solidified to minimise porosity, homogenised for 10 days at 520°C, and extruded at this same temperature into rod of 9.5 mm diameter at the British Aluminium Research Laboratories. Tensile specimens of 12.7 mm gauge length and 6.35 mm diameter were machined from this material.

A few supplementary experiments were performed on material which was very rapidly quenched from the melt to produce fine powder. This was compacted at room temperature and extruded at 300°C to produce rod of 5 mm diameter. Tensile specimens of 12.7 mm gauge length and 4.3 mm diameter were machined from this material.

Testing was carried out on an Instron testing machine (model TT-C-L) capable of various constant cross-head velocities between 0.847 $\mu\text{m s}^{-1}$ and 0.847 mm s^{-1} . A triple-wound furnace was used with a constant temperature zone ($\pm 2^\circ\text{C}$) approximately 130 mm long.

The strain-rate-sensitivity of the homogenised material was determined at 410, 450, 485 and

*Present address: The Weldless Steel Tube Co Ltd, Wednesfield, Staffs, UK.

520°C using a velocity-change technique in which a single specimen was subjected to a number of different constant velocities. The maximum stress (σ) attained at each velocity was determined (where possible) together with the instantaneous true strain-rate ($\dot{\epsilon}$) corresponding to this value of stress, assuming uniform reduction of the specimen. The strain-rate-sensitivity of the powder material was similarly determined at 370 and 450°C.

The variation of flow stress and microstructure with strain was more fully investigated at 520°C using nominally constant true strain-rates of 6×10^{-5} , 6×10^{-4} and $6 \times 10^{-3} \text{ s}^{-1}$. Constant true strain-rate was achieved by suitably modifying the Instron machine as described in the appendix.

After deformation the specimens were sectioned longitudinally and samples for metallographic examination prepared by conventional techniques. Some undeformed specimens which had been annealed for varying times at 520°C were similarly prepared. Etching in 10% NaOH solution for 2 sec at 70°C revealed the CuAl_2 particles in dark contrast. Grain boundaries in the aluminium-rich phase were shown up by over-etching ($\sim 4 \text{ s}$).

The mean transverse and longitudinal grain diameters were obtained in both the undeformed (grip) and deformed regions of the specimens by averaging not less than 100 grains per speci-

men (at a magnification of $\times 420$). The mean interphase separation distance was obtained from the same photographs using the lineal intercept method with lines drawn in both the transverse and longitudinal directions. At least 100 interceptions in each direction were counted. The true average grain diameter, D , and the average interphase separation, L , were evaluated from the corresponding values d and l measured on a planar section by means of the relations [16] $D = (4/\pi) d$, and $L = (16/\pi^2) l$.

3. Results

3.1. Mechanical

The values of σ and $\dot{\epsilon}$, calculated from the results of velocity-change experiments as detailed in section 2, were used to construct the $\log \sigma$ versus $\log \dot{\epsilon}$ plots of fig. 1. Maximum errors in σ and $\dot{\epsilon}$ are estimated to be $\pm 10\%$. The greater scatter of the results from the powder material arose from the less stable structure (see section 3.2). The curves for this material are drawn through those points separated by the shortest time intervals.

The different form of the curves is to be noted and can be correlated with microstructural differences between the two types of material (see section 3.2). The value of m obtained from the linear portion of the curves decreased with decreasing temperature, but was always in excess of 0.3 and, therefore, conducive to superplasticity [1]. The upper strain-rate limit for superplasticity (arbitrarily taken at the point where m falls to 0.3) in the homogenised material was increased by a factor of four on increasing the temperature from 410 to 520°C. The upper strain-rate limit in the powder material could not be determined but was at least 10^{-1} s^{-1} at 450°C. Elongations in excess of 1000% were obtained in both types of material under optimum conditions.

Fig. 2a shows the variation of flow stress with true strain (ϵ) at the three constant strain-rates used in this study. Each full symbol represents a value of stress, calculated as the final load divided by the minimum-cross-sectional area, obtained from a specimen deformed to the strain shown. The open symbols represent results from a single specimen which was removed from the furnace and measured at each strain indicated. The half-filled symbols represent stresses calculated assuming uniform reduction in area. This assumption has been shown to be valid up to strains of the order of 1.5.

At all three strain-rates the flow stress is

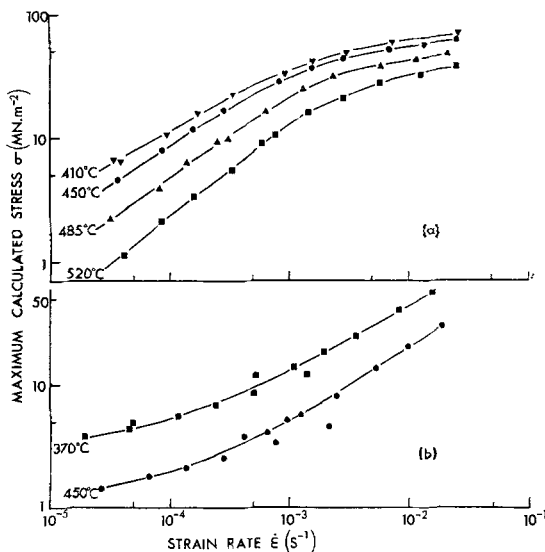


Figure 1 Logarithmic plot of flow stress against strain-rate for the Al-Cu eutectic. (a) Conventionally cast and homogenised. (b) Powder material.

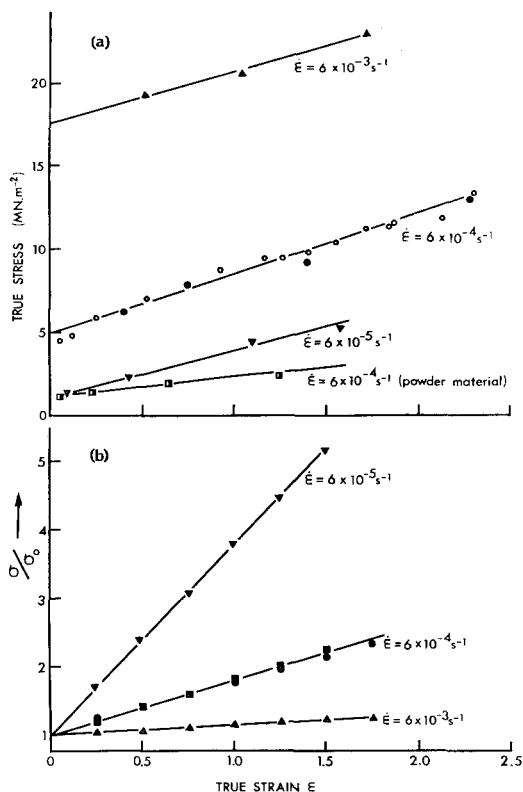


Figure 2 (a) Flow stress, and (b) (σ/σ_0) against true strain at constant true strain-rate. Temperature 520°C.

linearly related to strain. The lines can be back-extrapolated to give a value of stress, σ_0 , corresponding to zero plastic strain. σ_0 is a function of strain-rate and (see section 3.2) the initial microstructure. The slopes of the lines are similar for the homogenised material but clearly different for the powder material.

Fig. 2b is a plot of σ/σ_0 against true strain. The slope of the lines is inversely related to strain-rate and both materials at $6 \times 10^{-4} \text{ s}^{-1}$ follow a common curve. Thus the results obtained can be represented by the equation:

$$\sigma/\sigma_0 = 1 + k(\dot{\epsilon}) \epsilon \quad (1)$$

where $k(\dot{\epsilon})$ is a function of strain-rate, but is independent of initial microstructure.

The device used to maintain a constant true strain-rate could not allow for non-uniform reduction of the specimen. A tapered specimen was produced at $6 \times 10^{-4} \text{ s}^{-1}$ for $\epsilon > 1.4$ (300%) and at $6 \times 10^{-3} \text{ s}^{-1}$ for $\epsilon > 0.9$ (150%). Therefore, the true strain-rate measured as $-dA/dt$ (where A is the instantaneous cross-sectional

area) may have exceeded the stated constant value above these strains. This would cause an increase in flow stress, the magnitude of which is difficult to assess. The fact that the specimen was gradually tapered, rather than locally necked, and that the stress values lie on a reasonably good straight line suggest that the increase in stress due to this cause was small. The maximum strain-rate achieved would not have exceeded $1\frac{1}{2}$ times the stated constant value.

3.2. Microstructural

The as-extruded structure of the homogenised and of the powder materials is shown in figs. 3a and b respectively. There was a marked directionality of structure in the homogenised material with banding of the phases along the extrusion direction. The presence of many small CuAl_2 particles (dark phase) made the estimation of the mean interphase separation distance, L , difficult, but inspection of the photo-micrograph was sufficient to show that this distance would not be equal to the mean grain diameter of the Al-rich phase, particularly in a direction parallel to the extrusion axis. It is to be noted that the grain structure of the Al-rich phase did not exhibit any pronounced elongation in this direction. The grain diameter was $\sim 5 \mu\text{m}$.

The as-extruded powder material (fig. 3b) was composed of a mixture of degenerate and lamellar regions of varying, but extremely fine, interphase spacing. Some of the boundaries between dissimilar regions appeared to be the outlines of the original powder particles, elongated by the extrusion process.

The initial structures typified by figs. 3a and b were by no means stable at elevated temperatures. The most pronounced changes occurring in the homogenised material during short annealing times (of the order of the testing time) were solution of the smaller, fragmented CuAl_2 particles, coarsening of the larger CuAl_2 particles and an increase in the α -Al grain size. The banding of the structure was still in evidence. Longer annealing times (days) at 520°C resulted in a gradual coarsening of the structure, an increased angularity of the Al/ CuAl_2 interface and a reduction in the extent of the banding.

Annealing of the powder material at 520°C, even for very short times (~ 10 min) caused the lamellar regions to degenerate and removed the particle outlines. The structure was then comprised entirely of degenerate regions of varying inter-phase-separation. L increased with anneal-

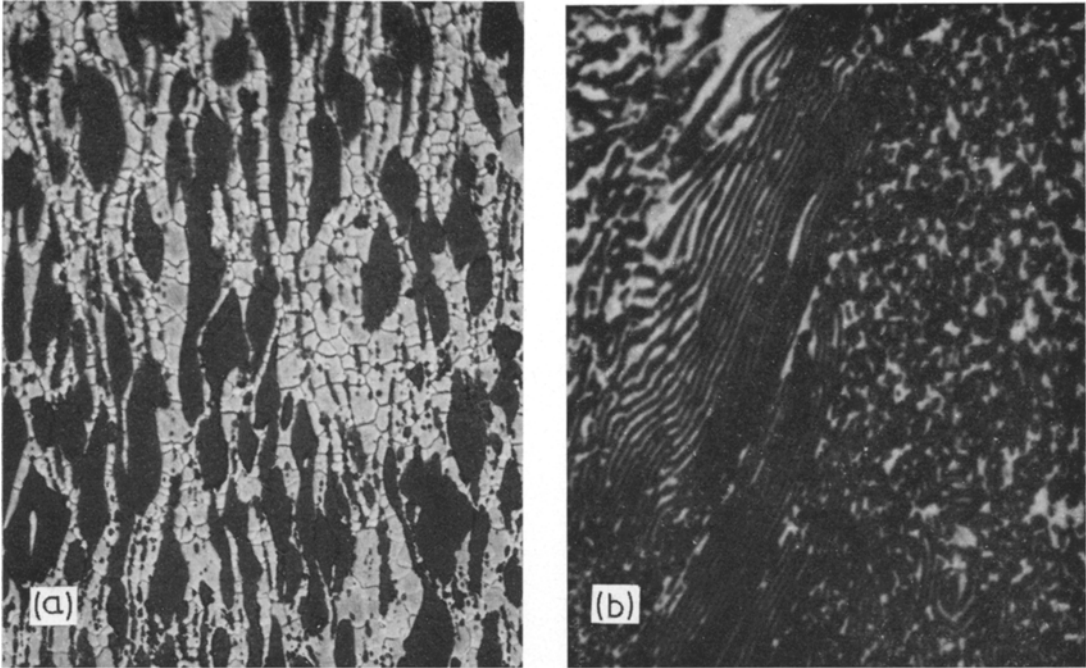


Figure 3 Microstructure of as-extruded material. Extrusion axis vertical. (a) Conventionally cast and homogenised ($\times 420$). (b) Powder material ($\times 840$).

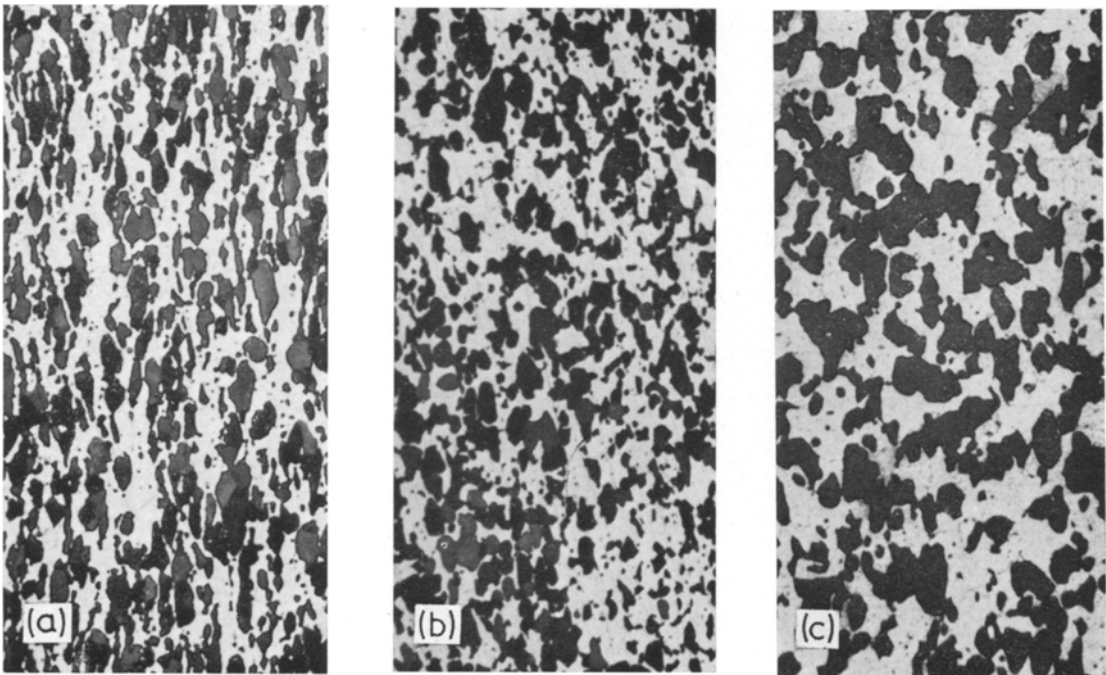


Figure 4 Microstructure of homogenised material, superplastically deformed at a constant true strain-rate of $6 \times 10^{-4} \text{ s}^{-1}$. Temperature 520°C ; tensile axis vertical ($\times 216$). (a) $\epsilon = 0$. (b) $\epsilon = 0.40$. (c) $\epsilon = 2.28$.

ing time and became more uniform throughout the structure. At 2 h it was $\sim 5 \mu\text{m}$. The $\alpha\text{-Al}$ grains could not be revealed by etching and so the grain diameter, D , was taken to be equal to L .

The microstructural changes accompanying superplastic deformation have been most closely studied at $6 \times 10^{-4} \text{ s}^{-1}$. Fig. 4 shows the changes in the homogenised material as a function of true strain ($\ln(A_0/A)$). Each micrograph was obtained from a separate specimen deformed to the strain shown. Fig. 4a is representative of a 30 min anneal. The time of testing of the other two specimens is given in the table. The annealed microstructure 4a still contained many small CuAl_2 particles whose number decreased as the strain increased. Deformation also produced a gradual removal of the banding up to $\epsilon \approx 1.4$. Thereafter, the only change appeared to be a coarsening of the microstructure. What seems more likely is that the relative movements of the two phases, which must occur to allow the specimen to change shape, were such that the microstructures always appeared similar. A change from a banded to a more equiaxed microstructure during superplastic deformation

has been reported previously by Morrison [12] and ourselves [14].

The change in microstructure of the powder material was observed on a single specimen deformed to failure ($\epsilon = 3.9$) at $6 \times 10^{-4} \text{ s}^{-1}$. The deformed specimen had a tapered cross-section and the microstructure varied along its length (fig. 5). Fig. 5a is the grip region of the specimen and is representative of a 60 min anneal. Deformation again produced coarsening of the microstructure fig. 5b and an increasing number of voids was observed near the fracture region fig. 5c.

It is interesting to note that the deformed microstructures of both types of material at large strains were of similar appearance even though the initial microstructures were very different.

The table summarises the quantitative measurements made on the homogenised material. The differences between grain diameters in the grip and in the deformed regions were never greater than $\sim 3 \mu\text{m}$ (20%) and only at $6 \times 10^{-5} \text{ s}^{-1}$ was the deformed grain diameter significantly larger than that in the grip. Thus, it appeared that the important factor governing the grain-size of the

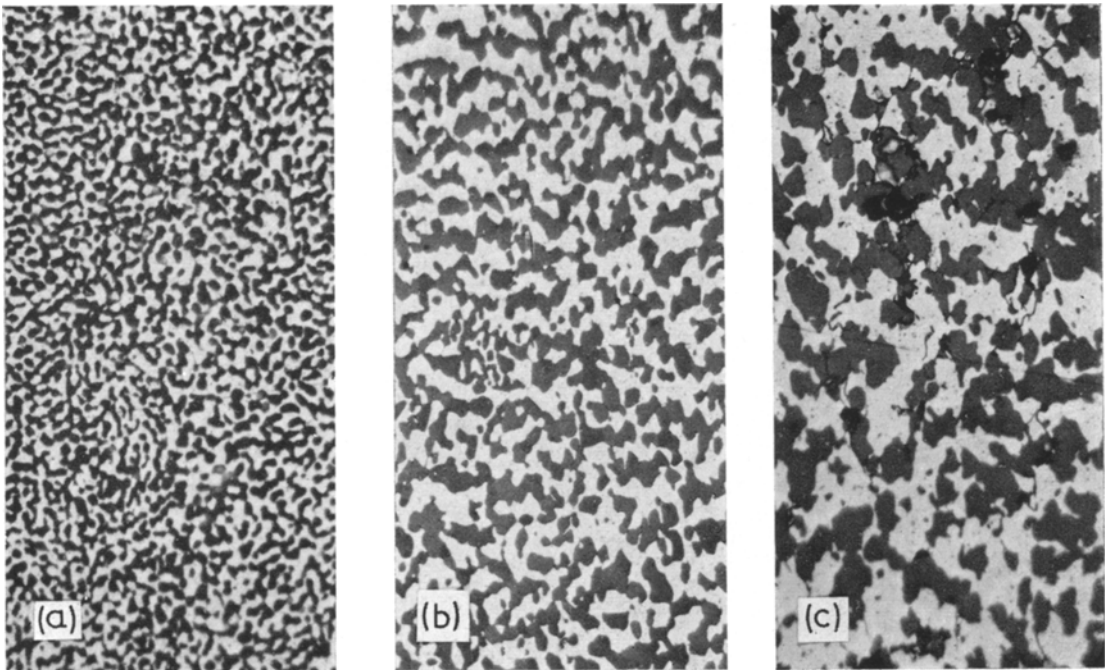


Figure 5 Microstructure of a single, tapered specimen of the powder material, superplastically deformed at a constant true strain-rate of $6 \times 10^{-4} \text{ s}^{-1}$. Temperature 520°C ; tensile axis vertical ($\times 420$). (a) $\epsilon = 0$. (b) $\epsilon \approx 1.8$. (c) $\epsilon = 3.9$.

True strain (ln A ₀ /A)	Testing time (min)	Mean inter-phase separation, L(μm)				Mean grain diameter, D(μm)				Strain-rate (s ⁻¹)
		Undeformed		Deformed		Undeformed		Deformed		
		L _⊥	L _∥	L _⊥	L _∥	D _⊥	D _∥	D _⊥	D _∥	
0	0	6.5	18.0			5.0	6.0			0
0.51	1.5	10.5	18.5	9.5	16.5	7.5	10.5	7.0	11.0	6 × 10 ⁻³
1.05	2.5	9.0	16.5	13.0	14.5	6.5	9.5	7.5	9.5	
1.83	4.0					6.5	9.5	7.5	9.0	
0.40	13.5	10.0	18.5	10.0	15.0	7.5	11.0	7.0	10.0	6 × 10 ⁻⁴
0.75	23.0	8.5	17.0	9.5	15.5	7.5	9.5	7.5	11.0	
1.42	34.5	10.5	16.5	12.5	19.5	7.5	11.0	7.5	11.5	
2.28	45.5			13.0	18.0	8.0	12.0	8.5	12.0	
3.57	56.5	11.5	21.0	15.5	23.0	7.5	10.5	8.5	12.5	
0	120	10.5	20.5			8.0	11.0			
0.43	143	13.5	23.5	14.5	19.5	9.0	12.0	10.0	14.5	6 × 10 ⁻⁵
1.09	320	15.0	30.0	15.5	25.0	11.0	14.5	12.0	18.0	
1.56	460	14.5	26.5	18.0	27.5	11.0	16.0	14.5	19.5	
0	2880	17.0	25.0			12.5	18.0			0
0	7200	16.5	30.0			15.0	20.5			
		Scatter in L ± 20%				Scatter in D ± 50%				

homogenised material was time at temperature and not strain. There was a significant difference between the grain-size of the as-extruded material and that reheated to 520°C for testing. Clearly, coarsening of the grains had occurred during the heating period, which was 40 min. This was particularly true parallel to the extrusion axis, in contrast with L where the most significant change during heating was perpendicular to the tensile axis. L_⊥ increased by 4 μm during the heating period but a further period of ten times this

duration was needed to produce a further coarsening of 4 μm. Deformation enhanced the increase in L_⊥ but did not lead to a significant increase in L_∥.

The ratios D_∥/D_⊥ and L_∥/L_⊥ in the homogenised material are plotted in fig. 6 against log (time). L_∥/L_⊥ fell rapidly from 2.8 in the as-extruded state to a constant value ~1.8 (undeformed) and 1.5 (deformed). D_∥/D_⊥ rose from 1.2 in the as-extruded state to ~1.5 (both undeformed and deformed). The powder material

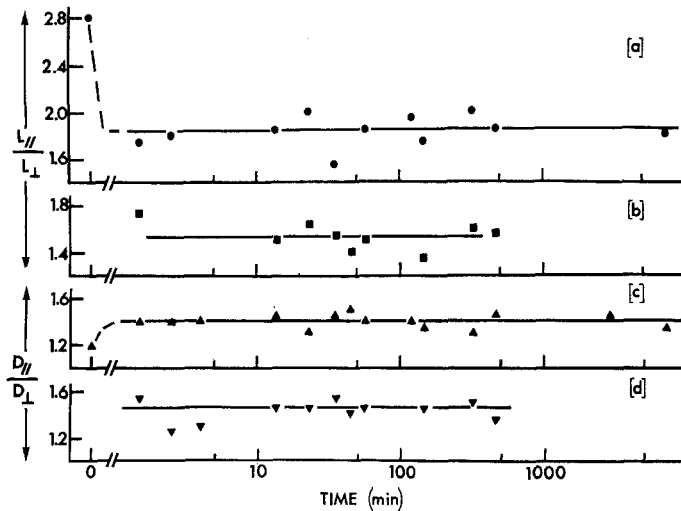


Figure 6 Anisotropy of microstructure of the homogenised material against log (time at 520°C) (a) (L_∥/L_⊥) undeformed. (b) (L_∥/L_⊥) deformed. (c) (D_∥/D_⊥) undeformed. (d) (D_∥/D_⊥) deformed.

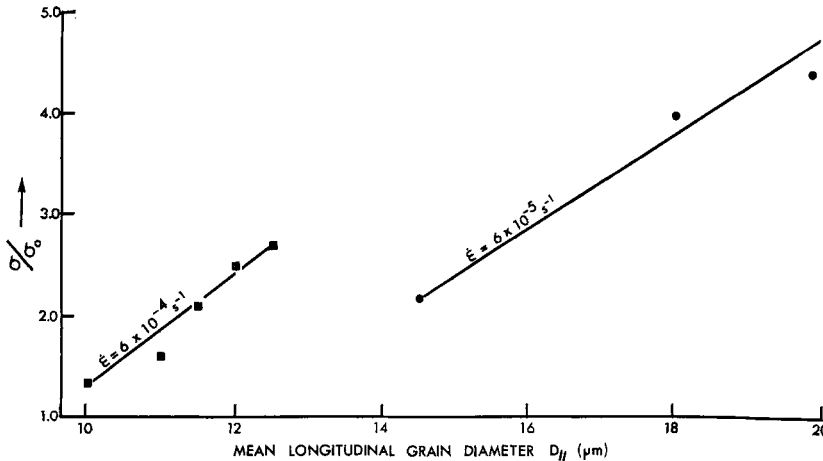


Figure 7 (σ/σ_0) against $D_{||}$ for the homogenised material deformed at $6 \times 10^{-4} \text{ s}^{-1}$ and $6 \times 10^{-5} \text{ s}^{-1}$ at 520°C .

retained an equiaxed microstructure in the undeformed state (ratio = 1.0) but both $D/D_{\perp||}$ and $L_{||}/L_{\perp}$ increased to ~ 1.5 in the deformed material.

From these results one may conclude that the deformed microstructure was not equiaxed, but exhibited an anisotropy in which the grain dimension in the longitudinal direction was 50% longer than that in the transverse direction. This anisotropy arose from deformation of both types of material studied, the one containing a banded two-phase microstructure and the other an equiaxed two-phase microstructure.

Fig. 7 is a plot of σ/σ_0 (obtained from fig. 2b) against $D_{||}$ (obtained from the table) for the two lower strain-rates used in this study. With the limited data available it would appear that σ/σ_0 is linearly related to $D_{||}$.

4. Discussion

Most of the work so far reported on superplastic alloys has employed constant velocity testing conditions to explore the stress-strain behaviour. Since, for constant cross-head velocity, the true strain-rate continuously decreases with strain, the influence of these two variables on superplastic deformation cannot be separated. This study, in which constant true strain-rates were achieved up to true strains ~ 1.4 to 1.8, has partially overcome this problem.

The results obtained in this study suggest that true steady-state, constant flow stress conditions are not obtained in the superplastic Al-Cu eutectic. Indeed, the material used exhibited

linear hardening over most of the strain range investigated, i.e.

$$(\sigma/\sigma_0) = 1 + k(\dot{\epsilon}) \epsilon$$

where the factor $k(\dot{\epsilon})$ is a strong function of strain rate, but is independent of the initial microstructure; the value of σ_0 is, however, dependent on microstructure (see fig. 2). We now discuss possible reasons for this strain-hardening behaviour.

Linear strain hardening is often exhibited by pure single crystals and polycrystals and can be explained on the basis of dislocation interactions. Such a mechanism can be ruled out on two accounts. Firstly, dislocation hardening is not very strain-rate-sensitive whereas the hardening observed here is (fig. 2b). Secondly, transmission electron microscopy of the deformed specimens has revealed very few dislocations within the α -Al grains, and the cellular dislocation substructures characteristic of hot-worked aluminium were not formed during superplastic deformation.

A second possibility is that non-uniform deformation [17] along the gauge length, leading to localised increases in true strain-rate, produced strain-rate hardening. This effect is undoubtedly of importance during the final stages of superplastic deformation when pronounced tapering along the gauge length occurs, but our measurements of the uniformity of deformation indicate that the effect is of minor significance over most of the strain range for which results were obtained.

A third, and most likely, explanation for the strain-hardening is that it is due to microstructural coarsening. It is well documented [2-10] that the flow stress of superplastic alloys is strongly dependent on the scale of the microstructure and this is shown in fig. 7 for our alloy. (σ/σ_0) increases approximately linearly with grain size, so we may conclude that the grain-size is proportional to natural strain. The influence of microstructural coarsening on flow stress is a factor which has not received much attention and can lead to erroneous estimates of strain-rate-sensitivities derived from velocity-change tests, as discussed by Hedworth and Stowell [18].

The metallographic evidence reported in section 3.2 is significant in two main respects. Firstly, both the inter-phase separation and the α -Al grain size have been measured. Secondly, the results of grain size measurement show that in this alloy equiaxed α -Al grains are not maintained during superplastic deformation, an observation which is contrary to all previous reports.

The initial as-extruded structure changes rapidly during deformation. In the homogenised material the almost equiaxed grain structure ($D_{\parallel}/D_{\perp} = 1.2$) becomes more anisotropic ($D_{\parallel}/D_{\perp} = 1.5$) due, most probably, to the dissolution of the small CuAl_2 particles in the α -Al matrix which inhibit grain growth parallel to the tensile axis; grain growth in the orthogonal direction is, of course, inhibited by the massive, banded CuAl_2 particles. Concurrently, the phase structure becomes less anisotropic, the ratio (L_{\parallel}/L_{\perp}) falling from 2.8 to ~ 1.5 (deformed) and 1.8 (undeformed). This is due to the breakdown of the longitudinally banded initial structure, as described previously [14]. The smaller anisotropy of the deformed material is probably an indication of stress enhancement of the diffusion-controlled breakdown process. In the powder material, the initial grain and phase structure is equiaxed when deformation starts and this structure is much more stable in the grip regions than in the gauge length where, again, anisotropy of the α -Al grains is produced ($D_{\parallel}/D_{\perp} \sim 1.5$). Here, a similar anisotropy of the phase distribution (L_{\parallel}/L_{\perp}) persists during deformation and the α -Al grain-size and shape are clearly controlled by the phase-structure.

The anisotropy of structure reported here contrasts with the results of Lindinger, Gibson, and Brophy [19] who made a quantitative study of superplastic deformation in a Ni-Fe-Cr alloy.

They reported four sets of measurements of grain anisotropy which gave (D_{\parallel}/D_{\perp}) values varying from 1.03 to 1.37, and concluded that the grain structure was essentially isotropic. The difference between their results and ours is worth discussing from the microstructural viewpoint.

The ability of a superplastic material to retain an approximately equiaxed grain structure must depend both on interface mobility and the extent of interface sliding. The term interface includes both inter-phase boundaries and grain boundaries. An important difference between the two alloys is the volume fraction of the second phase (~ 0.5 in the Al-Cu alloy and ~ 0.2 in the Ni-Fe-Cr alloy). For the same matrix grain-size, grain boundaries in the Ni-base alloy will have a greater area and will be more "flexible" than those in the Al-Cu alloy. The resistance to shear at inter-phase boundaries is probably greater than at matrix grain boundaries in both alloys but this is less important in the Ni-base alloy because the total inter-phase interface area is less and the matrix boundaries can more easily accommodate both the migration and sliding movements needed to produce an equiaxed grain shape. A second factor to consider is the relative plasticity of the co-existing phases. The γ -Ni and α -Cr based phases have similar hot plastic properties whereas CuAl_2 exhibits negligible ductility at $\sim 520^\circ\text{C}$ [20] compared with α -Al. The mobility of the inter-phase boundaries will depend upon the plastic properties of the harder phase so that this factor will also be important in determining the microstructural changes required to retain an equiaxed grain structure.

It was extremely difficult to obtain accurate measurements of D and L in samples prepared from powder material. However, it was clear that, at 520°C , very rapid natural coarsening of these very fine microstructures occurred and that deformation produced a proportionately greater increase in both grain-size and phase dispersion than in the conventionally cast and homogenised material. Consequently, the advantages of a fine, initial microstructure were rapidly lost. However, fig. 1 illustrates that the powder material was still superplastic at 370°C , where metallography indicated that the coarsening due to annealing was small in comparison with that produced by deformation. A recent report by Beghi *et al* [21] has demonstrated superplasticity in foils $\sim 50\mu\text{m}$ thick produced by splat-quenching an Al-17wt %Cu alloy. When tested in tension at 400°C this material elongated

600%. Although this alloy was not tested in bulk form, nevertheless it confirms that a fine-grained structure having a uniform dispersion of the two phases can be produced by rapidly quenching from the melt. With alloys that are difficult to produce in a fine-grained state by conventional methods, the powder route has much to recommend it and, in some systems, this may be a means of producing superplasticity at strain-rates that are high enough to allow commercial exploitation.

Acknowledgements

The technical assistance of Mr D. J. Baldwin and Mr D. G. E. Owen is gratefully acknowledged. Dr H. Jones and Mr M. H. Burden kindly provided the rapidly quenched material and their advice and assistance is much appreciated. We are grateful to British Aluminium Research Laboratories for providing extrusion facilities and to Dr D. A. Melford for his critical reading of the manuscript. This paper is published by permission of the Chairman of Tube Investments Limited.

Appendix

Constant Strain-rate Apparatus

If it is assumed that an initially cylindrical specimen deforms uniformly along its length in a tensile test, the true strain-rate, $\dot{\epsilon}$, is given by:

$$\dot{\epsilon} = (1/l) dl/dt = V/l \quad (\text{A1})$$

where l is the instantaneous specimen length and V is the relative velocity of the ends of the specimen. If $\dot{\epsilon}$ is to remain constant during testing, V must be continuously adjusted. The purpose of this appendix is to describe an attachment to an Instron Model TT-C-L testing machine which achieves this end.

In normal operation, this machine provides a range of constant cross-head velocities which may be altered by changing cogs in an externally-mounted gear box. The box contains an input drive shaft (D in fig. A1) which is powered by an internal motor, and an output shaft E which is connected via a servo system to the cross-head drive.

The constant strain-rate device is interposed between D and E, replacing the fixed gears by a system which allows the angular velocity of E and hence the cross-head speed to be continuously varied. The device is illustrated in fig. A1. The ball-bearing B transmits the drive between the disc A, radius R_a , and the shaft C, radius r_c ,

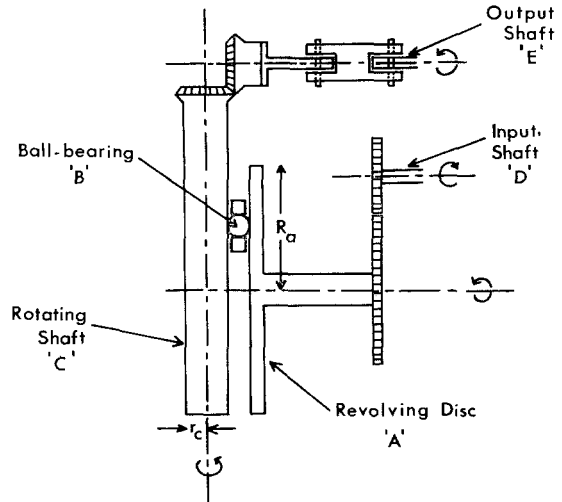


Figure A1 The position of the device.

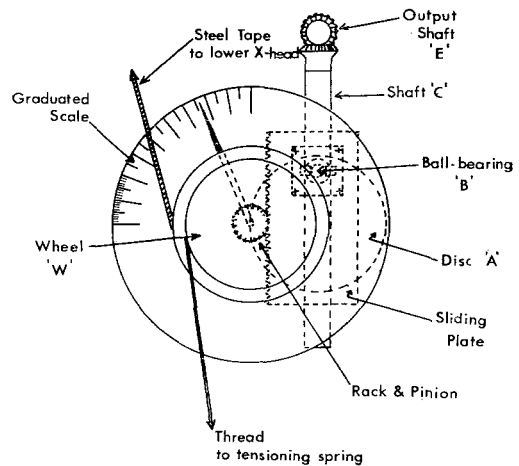


Figure A2 Front view of device.

and can be moved to any position from the centre to the edge of A. Thus, C can be given any velocity from zero (B at centre of A) to $V_c = \pm (R_a/r_c) V_a$ where V_a is the input velocity of A. The ball-bearing is mounted on a sliding plate (fig. A2) and it is positioned by rotating the wheel W, connected to the plate by a rack and pinion mechanism. Control and continuous adjustment of the cross-head speed is achieved by a steel tape which passes through a pulley system and is fixed to the lower cross-head at one end and to the wheel W at the other. Downward movement of the cross-head results in a clockwise rotation of the wheel W, displacing the ball-bearing B which, in turn, changes the

speed of the servo drive to the cross-head. A scale, graduated in $\frac{1}{2}^\circ$ intervals, registers the position of B relative to the centre of A; a rotation of $\pm 360^\circ$ moves B from the centre to the edge of A. The cross-head velocity is given by:

$$V_c = (X/360) (R_a/r_c) V_a \quad (A2)$$

where X is the scale reading in degrees.

From equation A1, it is seen that for $\dot{\epsilon}$ to be constant, X must be proportional to l . From the geometry of the device this will be the case provided the initial angular setting x_0 is chosen to be $(l_0/\pi D) \times 360^\circ$, where l_0 is the initial gauge length of the specimen and D is the diameter of the wheel W .

An alternative method of obtaining constant true strain-rate conditions with an Instron testing machine has recently been described [22], but the constancy of $\dot{\epsilon}$ was limited to total elongations $\sim 70\%$. The device described here allows constant true strain-rate conditions to be obtained at strains up to $\sim 900\%$ for a 12.7 mm gauge length and is, therefore, ideally suited to the testing of superplastic alloys.

References

1. W. A. BACKOFEN, I. R. TURNER, and D. H. AVERY, *Trans. Amer. Soc. Metals* **57** (1964) 980.
2. D. H. AVERY and W. A. BACKOFEN, *ibid* **58** (1965) 551.
3. P. J. MARTIN and W. A. BACKOFEN, *ibid* **60** (1967) 353.

4. T. H. ALDEN, *Acta Metallurgica* **15** (1967) 469.
5. D. LEE and W. A. BACKOFEN, *Trans. A.I.M.E.* **239** (1967) 1034.
6. T. H. ALDEN, *Trans. Amer. Soc. Metals* **61** (1968) 559.
7. W. ZEHR and W. A. BACKOFEN, *ibid* **61** (1968) 300.
8. A. KARIM and W. A. BACKOFEN, *Mat. Sci. Eng.* **3** (1968/69) 306.
9. D. L. HOLT, *Trans. A.I.M.E.* **242** (1968) 25.
10. A. BALL and M. M. HUTCHISON, *Met. Sci. J.* **3** (1969) 1.
11. H. W. HAYDEN and J. H. BROPHY, *Trans. Amer. Soc. Metals* **61** (1968) 542.
12. W. B. MORRISON, *ibid* **61** (1968) 423.
13. R. KOSSOWSKY and J. H. BECHTOLD, *Trans. A.I.M.E.* **242** (1968) 717.
14. M. J. STOWELL, J. L. ROBERTSON, and B. M. WATTS, *Met. Sci. J.* **3** (1969) 41.
15. D. L. HOLT and W. A. BACKOFEN, *Trans. Amer. Soc. Metals* **59** (1966) 755.
16. J. H. HENSLER, *J. Inst. Metals* **96** (1968) 190.
17. W. B. MORRISON, *Trans. A.I.M.E.* **242** (1968) 2221.
18. J. HEDWORTH and M. J. STOWELL, to be published.
19. R. J. LINDINGER, R. C. GIBSON, and J. H. BROPHY, *Trans. Amer. Soc. Metals* **62** (1969) 231.
20. G. MIMA, T. YAMANE, and C. HAYASHI, *J. Jap. Inst. Metals* **32** (1968) 224.
21. G. BEGHI, R. MATERA, and G. PIATTI, *J. Mater. Sci.* **5** (1970) 820.
22. E. P. LAUTENSCHLAGER and J. O. BRITAIN, *Rev. Sci. Instr.* **39** (1968) 1563.

Received 14 December 1970 and accepted 3 February 1971.